

Preparation of ferromagnetic binary alloy fine fibers by organic gel-thermal reduction process

SHEN Xiang-qian(沈湘黔), CAO Kai(曹 凯), ZHOU Jian-xin(周建新)

School of Materials Science and Engineering, Jiangsu University, Zhenjiang 212013, China

Received 11 September 2005; accepted 5 March 2006

Abstract: Ferromagnetic metal fibers with a high aspect ratio (length/diameter) are attractive for use as high performance electromagnetic interference shielding materials. Ferromagnetic binary alloy fine fibers of iron-nickel, iron-cobalt and cobalt-nickel were prepared by the organic gel-thermal reduction process from the raw materials of citric acid and metal salts. These alloy fibers synthesized were featured with a diameter of about 1 μm and a length as long as 1 m. The structure, thermal decomposition process and morphologies of the gel precursors and fibers derived from thermal reduction of the gel precursors were characterized by FTIR, XRD, TG/DSC and SEM. The gel spinnability largely depends on the molecular structure of metal- carboxylates formed during the gel formation. The gel consisting of linear-type structural molecules shows good spinnability.

Key words: organic gel-thermal reduction; ferromagnetic binary alloy fiber; spinnability; linear-type structural molecule

1 Introduction

Ferromagnetic metal fibers (Fe, Ni, Co and their alloys fibers) with small diameters showing anisotropic characteristics are attractive for use as fillers in polymer-matrix composite advanced electromagnetic interference (EMI) shielding and radar absorbing materials[1–3]. Due to the electromagnetic radiation at high frequencies only penetrates the near surface region of an electrical conductor, known as skin effect, the electric field of a plane wave penetrating a conductor drops exponentially with increasing depth into the conductor. The composite material having a conductive filler of metal fibers with a small diameter is more effective than that with a large diameter. For effective use of the entire cross section of metal fibrous fillers for EMI shielding or radar absorbing materials, the diameter of the metal fiber should be comparable to or less than the skin depth[1]. Therefore, the filler of magnetic metal fibers with a diameter of 1 μm or less and a high aspect ratio (fiber-length over fiber-diameter) is required technologically.

Many interests are focused on the development of preparation processing for ferromagnetic metal fine fibers. SHUI and CHUNG[4] synthesized nickel fibers with a diameter of 0.4 μm and a length of 100 μm by electroplating metal nickel on a carbon fiber. CHOU et

al[5] invented a method for synthesizing nickel fibers with a diameter ranging from submicron to microns and a length up to centimeters. The invention involves reducing nickel ions in an aqueous solution in the presence of a magnetic field or a surfactant by a reducing agent such as $\text{N}_2\text{H}_4\cdot\text{H}_2\text{O}$ at 80–100 $^\circ\text{C}$. ZHAO et al[6,7] also obtained submicron poly-crystalline iron fibers by reducing metal ions in an aqueous solution under a magnetic field. ICHIKI et al[8] used a vapor phase deposition method to form nickel filaments with diameter of 100 μm and length of 3 mm. However, these processing routes are considered expensive to make fine metal fibers and difficult to produce fine alloy fibers. The sol-gel method based on hydrolysis of alkoxide compounds is a promising approach for fine ceramic fibers. TSAI[9–11] prepared Mg_2SiO_4 fibers by the sol-gel process using $\text{Si}(\text{OC}_2\text{H}_5)_4$ and $\text{Mg}(\text{OCH}_3)_2$ as the starting reagents and found that the gel's spinnability was improved by addition of linear-type molecular citric acid. Although organic gel processes have been used to produce various ceramic oxide powders or coatings [12,13], few literatures about metal fibers prepared by this route have been previously reported[14]. The aim of this investigation is to determine the feasibility of utilizing the organic gel-thermal reduction process to prepare iron-nickel, iron-cobalt and nickel-cobalt fine alloy fibers from the raw materials of citric acid and

metal salts.

2 Experimental

2.1 Preparation of metal fibers

The starting reagents were citric acid ($\text{C}_6\text{H}_7\text{O}_5 \cdot \text{H}_2\text{O}$, AR), iron nitrate ($\text{Fe}(\text{NO}_3)_3 \cdot 9\text{H}_2\text{O}$, AR), cobalt nitrate ($\text{Co}(\text{NO}_3)_2 \cdot 6\text{H}_2\text{O}$, AR), nickel basic carbonate ($\text{NiCO}_3 \cdot \text{Ni}(\text{OH})_2 \cdot 4\text{H}_2\text{O}$, AR). The metal salts and citric acid were dissolved in deionized water and diluted to form 0.2 mol/L aqueous solutions, respectively. According to the required composition, two metal salt solutions were then gradually added into the citric acid solution with continuous magnetic stirring. The final solution was magnetically stirred for 18–20 h at room temperature and was transferred to a rotary evaporator and evaporated in a vacuum at 60–70 °C to remove surplus water until a viscous liquid was obtained. The resultant liquid was then poured into an evaporating basin and heated in vacuum at 75 °C until a spinnable gel could be used for drawing gel fibers by handling a glass rod. The spinning performance of the gel was estimated from the capability of fiber formation by immersing a glass rod of about 2 mm in diameter into the gel and then pulling it up by hand.

The gel fibers were drawn from the spinnable gels and dried in vacuum at 80 °C for about 10 h. The dried gel fibers were then put in a quartz crucible and subsequently reduced into metal fibers under an atmosphere of N_2 (80%, volume fraction) and H_2 (20%, volume fraction) with total gas flow rate of 200 cm^3/min for 1 h at appropriate temperatures.

2.2 Characterization of fibers

The structure, composition and morphologies of the gel precursors and the products derived from thermal reduction of the precursors at different temperatures were examined by Fourier transform infrared spectroscopy (FTIR) using a model of Nexu670 spectrometer, X-ray diffractometry (XRD) using a D/max2500PC diffractometer (RIGAKU), and scanning electron microscopy using a JXA-840A instrument (JEOL). The decomposition process was investigated by thermo-gravimetric (TG) analysis and differential scanning calorimetry (DSC) using a SDT2960 (TA) system.

3 Results and discussion

3.1 Formation of gel precursors and their spinning performances

Fig.1 shows the XRD patterns of the iron-nickel, iron-cobalt and nickel-cobalt citrate gel precursors. It can be seen that these gel precursors are amorphous and do not contain crystalline inorganic salts. The FTIR spectra

and peak positions for the gel precursors shown in Fig.2 confirm the formation of complexes between $\text{Ni}^{2+}/\text{Fe}^{3+}$ ions, $\text{Fe}^{3+}/\text{Co}^{2+}$ ions, $\text{Ni}^{2+}/\text{Co}^{2+}$ ions and citric acid. The $\text{C}=\text{O}$ peak at 1 720 cm^{-1} corresponding to the pure citric acid shifts to 1 618 and 1 385 cm^{-1} for Fe-Ni-citrate, 1 617 cm^{-1} and 1 384 cm^{-1} for Fe-Co-citrate, 1 617 and 1 383 cm^{-1} for Ni-Co-citrate. The two bands at 1 350–1 650 cm^{-1} result from the $\text{C}=\text{O}$ symmetrical and asymmetrical stretching vibration, which are the characteristic absorption peaks for the citrates. This was indicative of the complex formation. The carbonyl peak at 1 720 cm^{-1} could be attributed to surplus citric acid or dissociative carbonyl contained in the gel precursors.

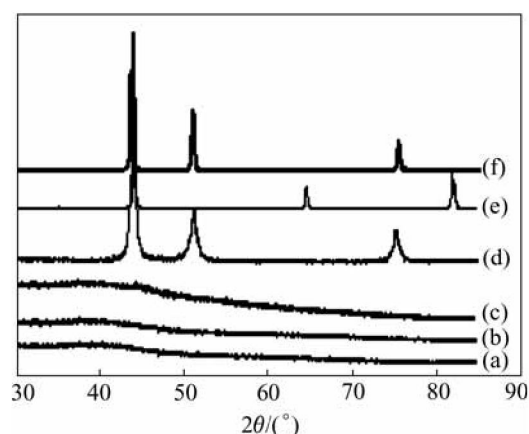


Fig.1 XRD patterns of gel precursors and products derived from thermal reduction of precursors: (a) FeNi precursor; (b) FeCo precursor; (c) CoNi precursor; (d) FeNi; (e) FeCo; (f) CoNi

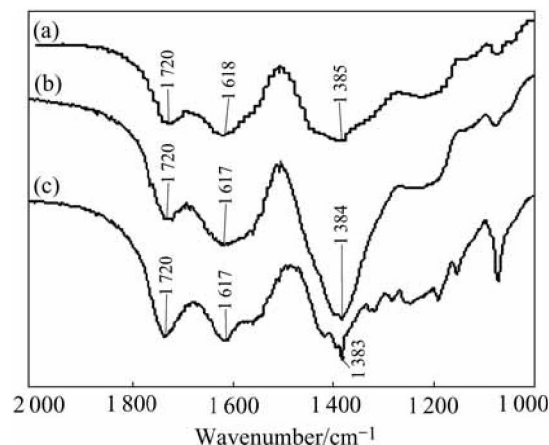


Fig.2 FTIR data for gel precursors: (a) Ferric-nickel citrate gel; (b) Ferric-cobalt citrate gel; (c) Cobalt-nickel citrate gel

According to Ref.[15], there are three possible liganding types between carboxylate and metal ions. It is believed that the single-dentate liganding leads to the formation of linear molecular structures and that the other two liganding types are beneficial to the net-work

molecular structures between metal ions and carboxylate. The value $\Delta\nu$ ($\Delta\nu=\nu_a-\nu_s$) can be used to classify the liganding type: the single-dentate corresponds to a higher value $\Delta\nu$, the double-dentate corresponds to a lower value $\Delta\nu$ and the bridge corresponds to an approximately equal value $\Delta\nu$ of the C=O in the complex compared to the free carboxylate. So that, referring to the value $\Delta\nu$ obtained from the FTIR data as listed in Table 1, the single-dentate between the metal ions and citric acid would be dominative and a linear molecular structure formed as shown in Fig.3.

Table 1 Characteristic frequency of FTIR spectra for various gel precursors

Gel precursor	$\nu_a(\text{C=O})/\text{cm}^{-1}$	$\nu_s(\text{C=O})/\text{cm}^{-1}$	$\Delta\nu/\text{cm}^{-1}$
Fe-Ni citrate gel	1 618	1 385	233
Fe-Co citrate gel	1 617	1 384	233
Ni-Co citrate gel	1 617	1 383	234

Table 2 shows the effects of chemical compositions on the gel spinnability. The iron-nickel citrate gel and iron-cobalt citrate gel exhibit good spinning performance when the molar ratio (R_a) is 1:1:1.8, which is close to the theoretical molar ratio of 1:1:5/3 for the molecular structures shown in Figs.3(a) and 3(b). The complexes

Table 2 Effect of different molar ratio on gel spinnability

Sample	R_a	Spinnability		
		Fe-Ni citrate gel	Fe-Co citrate gel	Ni-Co citrate gel
1	1:1:1	No	No	No
2	1:1:1.5	Short fiber	Short fiber	Short fiber
3	1:1:1.8	Long fiber	Long fiber	Short fiber
4	1:1:2.2	Short fiber	Short fiber	Long fiber
5	1:1:3	Short fiber	Short fiber	Short fiber

R_a for molar ratio for a, b and c; a and b for different metal ions; c for citric acid

for citric acid and $\text{Ni}^{2+}/\text{Co}^{2+}$ ions might exist in the form of molecular structures as shown in Figs.3(c) or 3(d) in the nickel-cobalt citrate gel, the molar ratio in the molecular structure as shown in Fig.3(c) is 1:1:4/3 and 1:1:2 in Fig.3(d), respectively. The nickel-cobalt citrate gel shows the best spinning performance when (R_a) is 1:1:2.2. The results suggest that the nickel-cobalt citrate complexes exist more probably in the form of molecular structure as shown in Fig.3(d) and this linear molecular structure is theoretically unlimited in length due to the bridging behavior of Ni^{2+} and Co^{2+} ions.

3.2 Thermal decomposition of gel precursors

Fig.4 shows the TG/ DSC curves of the various gel precursors. For all the compositions investigated, the thermal decomposition behaviors are similar and the thermal decomposition occurs according to the following four stages.

1) At 50–150 °C, the TG/DSC data exhibits a broad endothermic event corresponding to a mass loss of about 10%. This is attributed to the loss of free water and bound water in the gels.

2) At 150–250 °C, a large and sharp exothermic peak at around 180 °C occurred and accompanied a mass loss of 45%–50%. This is owing to the initial break-down of the complexes and spontaneous combustion. The increase in the ratio of nitrate to citrate would lead to an increase of the spontaneous combustion, because the nitrate ions provide an in situ oxidizing environment for the combustion of the organic component[16]. The molar ratios of nitrate to citrate in the iron-nickel citrate, iron-cobalt citrate and nickel-cobalt citrate gel precursors are 3:1.8, 5:1.8 and 1:1.1, respectively. Therefore, the exothermic event due to the spontaneous combustion of the iron-cobalt citrate gel is the most intensive.

3) At 250–380 °C, the gel decomposition experienced a mass loss of 10%–20%. The mass loss is caused by the decomposition of organic residues. The

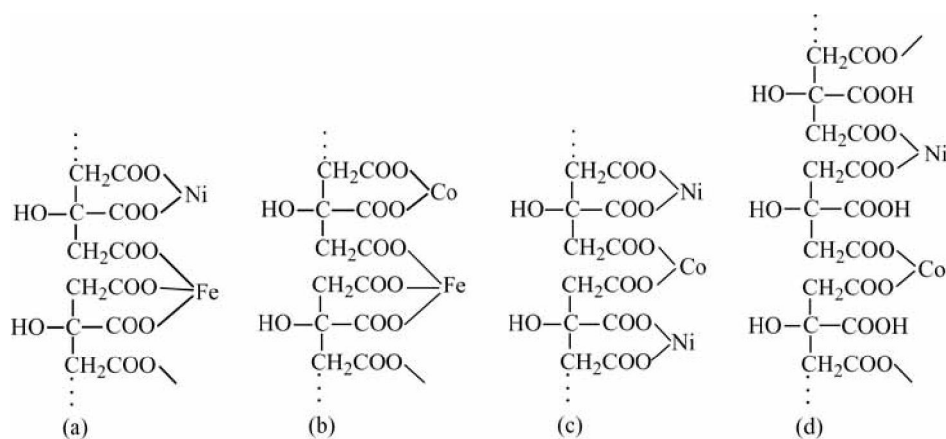


Fig.3 Possible molecular structures for various gel precursors: (a) $(\text{C}_6\text{H}_5\text{O}_7)_5(\text{FeNi})_3$ for Fe-Ni fibers; (b) $(\text{C}_6\text{H}_5\text{O}_7)_5(\text{FeCo})_3$ for Fe-Co fibers; (c) $(\text{C}_6\text{H}_5\text{O}_7)_4(\text{NiCo})_3$; (d) $[(\text{C}_6\text{H}_5\text{O}_7)_2\text{NiCo}]_n$ for Co-Ni fibers

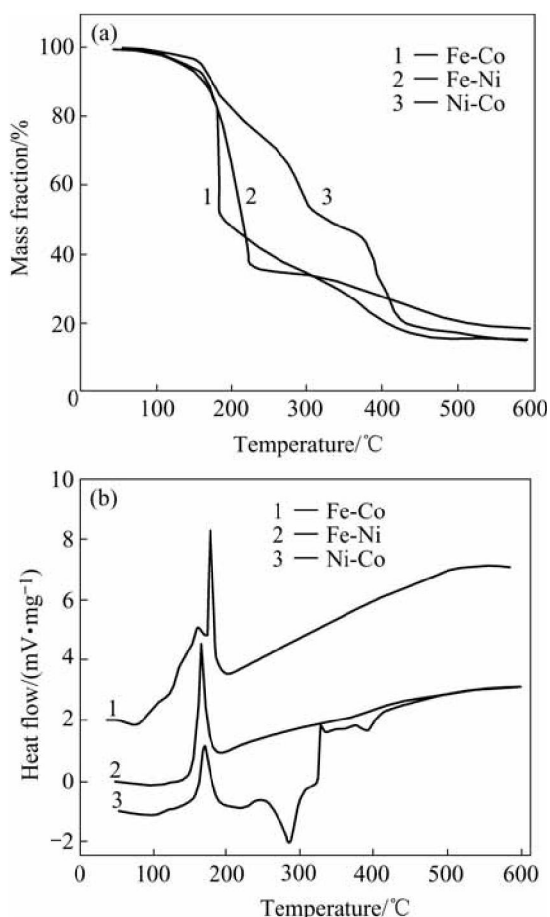


Fig.4 TG(a) and DSC(b) curves for gel precursors

nickel-cobalt citrate gel exhibits a sharp endothermic peak at about 280 °C, while no obvious endothermic event occurs around this temperature range for the other two gel precursors.

4) At 380–500°C and over, the mass loss decreases substantially. It is believed that this decomposition stage comprised of further oxidation of the residual carbon and formation of the metal oxides compounds. The little endothermic peak at about 400 °C for the nickel-cobalt citrate gel might be attributed to the formation of nickel-cobalt oxide solution[17,18].

According to the above analysis, the maximum temperature for the thermal decomposition-reduction of the gel fibrous precursors to form alloy fibers should be over 500 °C.

3.3 Characterization of metal fibers

The morphologies and microstructures of the ferromagnetic alloy fibers were affected by the processing parameters. The defects in the alloy fibers such as crack, surface roughness, porous and cone structures might occur during the dehydration and subsequent thermal reduction processes. By optimizing the processing parameters such as heat treatment programme and flow rate of the reduction gases, these

fiber defects can be eliminated. Fig.5 shows the surface morphologies of Fe-Ni alloy fibers at various thermal reduction temperatures. The increase of the reduction temperature led to the elimination of cracks and the increase of crystalline size, while large crystalline sizes have adverse effect on magnetic properties of the resultant fibers. Similar results are also obtained for iron-cobalt and nickel-cobalt alloy fibers in the thermal reduction process. The maximum temperature of 650 °C for the thermal decomposition-reduction of the gel fibrous precursor was used to form alloy fibers at a heating rate of 5 °C/min under atmosphere of N₂ (80%, volume fraction) and H₂ (20%) with total gas flow rate of 200 cm³/min for 1 h.

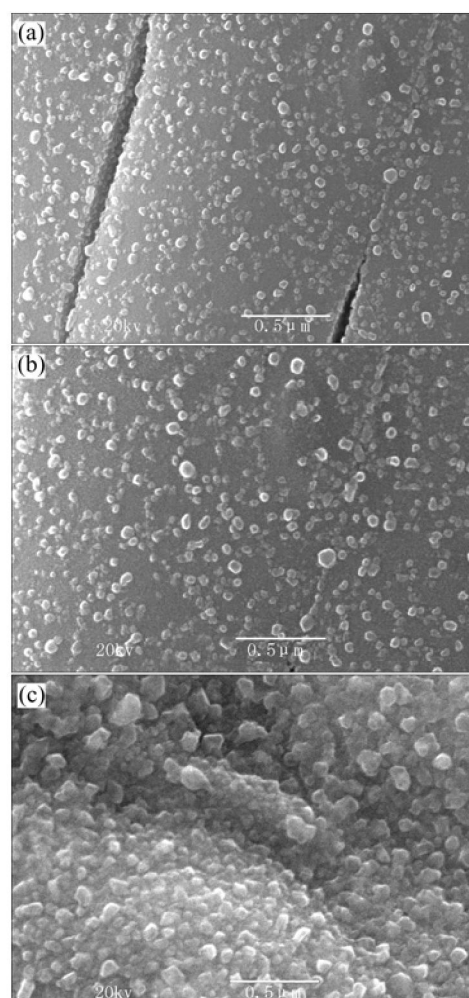


Fig.5 Effect of thermal reduction temperature on surface morphologies of Fe-Ni alloy fibers: (a) 500 °C for 1 h; (b) 650 °C for 1 h; (c) 800 °C for 1 h

After heat-treatment at 650 °C for 1 h, the iron-nickel (Fe₅₀Ni₅₀) alloy (JCPDS47-1417), iron-cobalt (Fe₅₀Co₅₀) alloy (JCPDS49-1567) and nickel-cobalt (Ni₅₀Co₅₀) solid solution (JCPDS04-0850) structural fibres were obtained (Figs.1(d), (e), (f)) and Fig.6 shows

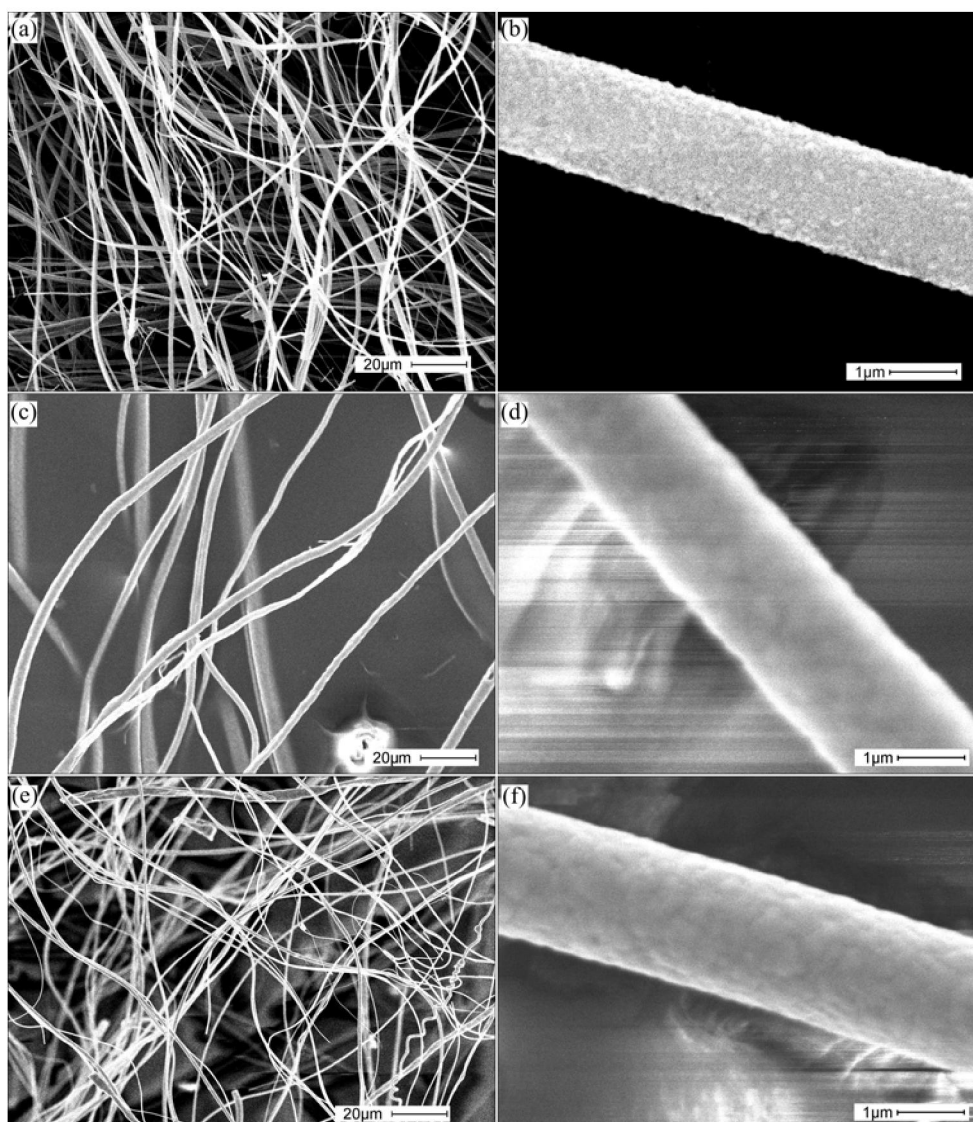


Fig.6 Morphologies of ferromagnetic binary alloy fibers: (a), (b) Fe-Ni alloy fibers; (c), (d) Fe-Co alloy fibers; (e), (f) Co-Ni alloy fibers

the morphologies of the alloy fibers with various diameters derived from the corresponding gel precursors under the above processing conditions. These alloy fibers are smooth and dense in surface, and have about 1 μm in diameter and 1 m in length.

4 Conclusions

1) The organic gel-thermal reduction process was successfully used for the preparation of ferromagnetic binary alloy Fe-Ni, Fe-Co, Ni-Co fine fibers with high aspect ratios using citric acid and metal salts as the starting reagents. The gel spinnability was related to the metal-carboxylate complex structure. The linear-type structural molecules $[(\text{C}_6\text{H}_5\text{O}_7)_5(\text{NiFe})_3]$ for the iron-nickel citrate gel, $(\text{C}_6\text{H}_5\text{O}_7)_5(\text{FeCo})_3$ for the iron-cobalt

citrate gel, $[(\text{C}_6\text{H}_5\text{O}_7)_2\text{NiCo}]_n$ for the nickel-cobalt citrate gel were possibly formed during reactions between citric acid and the corresponding metal ions. As a result, these gels exhibit a good spinning performance.

2) The fibrous gel precursors with the designed composition were correspondingly transferred into the ferromagnetic binary alloy fibers during the thermal reduction process at 650 $^{\circ}\text{C}$ under atmosphere of N_2 (80%) and H_2 (20%) with total gas flow rate of 200 cm^3/min for 1 h. These alloy fibers with diameter of about 1 μm and length of 1 m were smooth and dense. These ferromagnetic binary alloy fibers may be promising for applications in high performance conductive polymermatrix composites of electromagnetic interference(EMI) shielding and electromagnetic wave absorbing materials due to potential

anisotropic electric and magnetic properties.

References

- [1] CHUNG D D L. Materials for electromagnetic interference shielding [J]. *Journal of Materials Engineering and Performance*, 2000, 9(3): 350–354.
- [2] LI Yi, SHEN Guo-zhu, XU Zheng. Development of radar absorbing fibers in composites [J]. *Advanced Ceramics*, 2005, 1: 24–29.
- [3] ZHAO Zhen-sheng, ZHANG Xiu-cheng, NIE Yan. Microwave magnetic properties of polycrystalline iron fiber absorbing materials [J]. *J Magnetic Materials and Devices*, 2000, 31(1): 18–20.
- [4] SHUI X P, CHUNG D D L. Submicron diameter nickel filaments and their polymer-matrix composites [J]. *J Mater Sci*, 2000, 35(7): 1773–1785.
- [5] CHOU K S, REN C Y, LO C T. Method of Synthesizing Nickel Fibers and the Nickel Fibers so Prepared [P]. US 6375703B1, 2002.
- [6] ZHAO Zhen-sheng, WU Ming-zhong, HE Hua-hui. Preparation of magnetic and metallic fibers with reducing method of aqueous solution introduced by magnetic field [J]. *J Huazhong Univ of Sci & Tech*, 1998, 26(7): 74–76.
- [7] NIE Yan, ZHAO Zhen-sheng, HE Hua-hui. Polycrystalline iron fibers prepared by pyrolysis of carbonyl by introducing magnetic field [J]. *J Huazhong Univ of Sci & Tech*, 2001, 29(7): 75–77.
- [8] ICHIKI M, AKEDO J, MORI K, ISHIKAWA Y. Microstructure of nickel whiskers produced by the gas deposition method [J]. *J Mater Sci Lett*, 1997, 16: 531–533.
- [9] TSAI M T. Preparation and crystallization of forsterite fibrous gels [J]. *Journal of the European Ceramic Society*, 2003, 23: 1283–1291.
- [10] TSAI M T. Effects of hydrolysis processing on the character of forsterite gel fibers (Part II): Crystallites and molecular structure [J]. *Journal of the European Ceramic Society*, 2003, 22(7): 1073–1083.
- [11] TSAI M T. Effects of hydrolysis processing on the character of forsterite gel fibers (Part I): Preparation, spinnability and molecular structure [J]. *Journal of the European Ceramic Society*, 2002, 22(7): 1085–1094.
- [12] HODGSON S N B, SHEN X, SALE F R. Preparation of alkaline earth carbonates and oxides by edta-gel method [J]. *Journal of Materials Science*, 2000, 35: 5275–5282.
- [13] HODGSON S N B, SHEN X, SALE F R. Electrophoretic deposition of alkaline earth-edta complexes [J]. *Journal of Materials Science*, 2002, 37: 4018–4028.
- [14] SHEN Xiang-qian, JING Mao-xiang, WANG Tao-ping. Preparation of micrometer fibers by the organic-gel method [J]. *Journal of Inorganic Materials*, 2005, 20(4): 821–826.
- [15] TIMOTHY J S, SATISHI C B M. Speciation of aqueous Ni(II)-carboxylate and Ni(II)-fulvic acid solutions: combined ATR-FTIR and XAFS analysis [J]. *Geochim Cosmochim Acta*, 2004, 68(17): 3441–3458.
- [16] WU K H, YU C H, CHANG Y C. Effect of pH on the formation and combustion process of sol-gel auto-combustion derived NiZn ferrite/SiO₂ composites [J]. *Journal of Solid State Chemistry*, 2004, 177: 4119–4125.
- [17] VIAU G, FIEVET V F, FIEVET F. Nucleation and growth of bimetallic CoNi and FeNi monodisperse particles prepared in polyols [J]. *Solid State Ionics*, 1996, 4: 259–270.
- [18] ZENG Jing-hui, ZENG Huan-xing. Preparation of cobalt-based fine alloy powders and magnetic properties [J]. *Information Recording Materials*, 2001, 2(2): 6–8.

(Edited by LONG Huai-zhong)